

## Study of inverse Ni-based photonic crystal using the microradian X-ray diffraction

Vasilieva, A. V.; Grigoryeva, N. A.; Mistonov, A. A.; Sapoletova, N. A.; Napolskii, K. S.; Eliseev, A. A.; Lukashin, A. V.; Tretyakov, Yu D.; Bouwman, W. G.; More Authors

**DOI**

[10.1088/1742-6596/247/1/012029](https://doi.org/10.1088/1742-6596/247/1/012029)

**Publication date**

2010

**Document Version**

Final published version

**Published in**

Journal of Physics: Conference Series

**Citation (APA)**

Vasilieva, A. V., Grigoryeva, N. A., Mistonov, A. A., Sapoletova, N. A., Napolskii, K. S., Eliseev, A. A., Lukashin, A. V., Tretyakov, Y. D., Bouwman, W. G., & More Authors (2010). Study of inverse Ni-based photonic crystal using the microradian X-ray diffraction. *Journal of Physics: Conference Series*, 247, Article 012029. <https://doi.org/10.1088/1742-6596/247/1/012029>

**Important note**

To cite this publication, please use the final published version (if applicable).  
Please check the document version above.

**Copyright**

Other than for strictly personal use, it is not permitted to download, forward or distribute the text or part of it, without the consent of the author(s) and/or copyright holder(s), unless the work is under an open content license such as Creative Commons.

**Takedown policy**

Please contact us and provide details if you believe this document breaches copyrights.  
We will remove access to the work immediately and investigate your claim.

**OPEN ACCESS**

## Study of Inverse Ni-based Photonic Crystal using the Microradian X-ray Diffraction

To cite this article: A V Vasilieva *et al* 2010 *J. Phys.: Conf. Ser.* **247** 012029

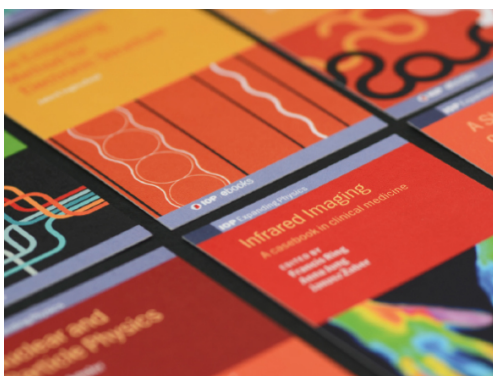
View the [article online](#) for updates and enhancements.

### Related content

- [Photonic crystals based on opals and inverse opals: synthesis and structural features](#)
- [Revealing stacking sequences in inverse opals by microradian X-ray diffraction](#)
- [Two-dimensional spatially ordered arrays of cobalt nanowires: polarized SANS study](#)

### Recent citations

- [Periodic order and defects in Ni-based inverse opal-like crystals on the mesoscopic and atomic scale](#)  
A. V. Chumakova *et al*



**IOP | ebooks™**

Bringing together innovative digital publishing with leading authors from the global scientific community.

Start exploring the collection—download the first chapter of every title for free.

## Study of Inverse Ni-based Photonic Crystal using the Microradian X-ray Diffraction

A V Vasilieva<sup>1</sup>, N A Grigoryeva<sup>2</sup>, A A Mistonov<sup>2</sup>, N A Sapoletova<sup>3</sup>, K S Napolskii<sup>3</sup>, A A Eliseev<sup>3</sup>, A V Lukashin<sup>3</sup>, Yu D Tretyakov<sup>3</sup>, A V Petukhov<sup>4</sup>, D Byelov<sup>4</sup>, D Chernyshov<sup>5</sup>, A I Okorokov<sup>1</sup>, W G Bouwman<sup>6</sup> and S V Grigoriev<sup>1</sup>

1 Petersburg Nuclear Physics Institute, Gatchina, 188350, St. Petersburg, Russia

2 Department of Physics, St. Petersburg State University, 198504, St. Petersburg, Russia

3 Department of Materials Science, Moscow State University, 119899, Moscow, Russia

4 Debye Institute, Utrecht University, 3584 CH Utrecht, the Netherlands

5 SNBL European Synchrotron Radiation Facility (ESRF), 38043 Grenoble, France

6 Delft Technical University, 2629 JB Delft, the Netherlands

E-mail: vasilieva@lns.pnpi.spb.ru

**Abstract.** Inverse photonic nickel-based crystal films formed by electrocrystallization of metal inside the voids of polymer artificial opal have been studied using the microradian X-ray diffraction. Analysis of the diffraction images agrees with an face-centred cubic (FCC) structure with the lattice constant  $a_0 = 650 \pm 10$  nm and indicates two types of stacking sequences coexisting in the crystal (twins of ABCABC... and ACBACB... ordering motifs), the ratio between them being 4:5. The transverse structural correlation length  $L_{tran}$  is  $2.4 \pm 0.1$   $\mu$ m, which corresponds to a sample thickness of 6 layers. The in-plane structural correlation length  $L_{long}$  is  $3.4 \pm 0.2$   $\mu$ m, and the structure mosaic is of order of  $10^\circ$ .

### 1. Introduction

Artificial opals consisting of submicron monodisperse microspheres packed in a face-centered cubic structure and materials on their basis are good candidates for the creation of high quality Photonic Crystals (PhC). They have recently attracted great attention due to their unusual optical properties and promising applications in optical devices. Inverse opals can be synthesized by filling the voids of opal templates and subsequent removing the initial microspheres. Three-dimensionally ordered porous

materials are thus obtained. One of the most promising methods of filling the voids is electrodeposition of metal, which enables almost 100% filling. The conducting PhC are of great interest from the viewpoint of multi-functionality and interplay between the optical, magnetic, and electronic transport properties.

The present study is aimed to investigate the structure of the inverse metallic PhCs deposited onto a conductive substrate. The important parameters of this technology are the substrate material, the surface roughness and the potential applied to the substrate. It has been established that PhCs synthesized by the vertical deposition method are often ordered in a face-centred cubic (FCC) structure [1]. However, they are prone to stacking disorder, which may result in the formation of a Random Hexagonal Close Packed (RHCP) structure with almost equal chances of finding FCC and hexagonal close-packed (HCP) stacking sequences [2]. Since photonic properties are based on the light interference phenomena, they may be strongly affected by structural disorder. It is difficult, however, to characterize and manipulate the degree of order. One of important properties of any crystal is the size and shape of structurally coherent blocks; technologically wise these properties describe an effective size of structurally ordered optical device. In this paper we characterize Ni-filled inverse crystal in terms of average structure and also give an estimate of its structural coherence.

## 2. Synthesis of Samples

The synthesis of samples was performed by a templating technique. At first the colloidal crystal films were formed from monodisperse polystyrene microspheres of  $\sim 450 \pm 10$  nm on the mica substrates with a thin thermally evaporated Au layer. Colloidal crystals were deposited at 60 °C from water suspension using the electric-field-assisted vertical deposition technique [2, 3]. During the crystal growth, the electric field of  $\sim 0.5$  V/sm was applied perpendicular to the substrates; as it has been shown in [2], this option allows formation of high-quality photonic crystals. At the second step the voids between the spheres were filled with nickel by electrochemical deposition. To control the filling of voids with metal, the electrodeposition was carried out in the potentiostatic mode at a voltage of -0.9 V relative to the Ag/AgCl reference electrode from the electrolyte having the following composition: 0.1M NiCl, 0.6M NiSO<sub>4</sub>, 0.1M H<sub>3</sub>BO<sub>4</sub>, 4M C<sub>2</sub>H<sub>5</sub>OH. To obtain the inverse structure, the polystyrene spheres were dissolved in toluene during 3 hours.

The preliminary characterization of samples was carried out using the scanning electron microscopy. Figure 1 shows the typical images of the obtained inverse PhC. Panels (a) and (b) represent top view and cross section, respectively.

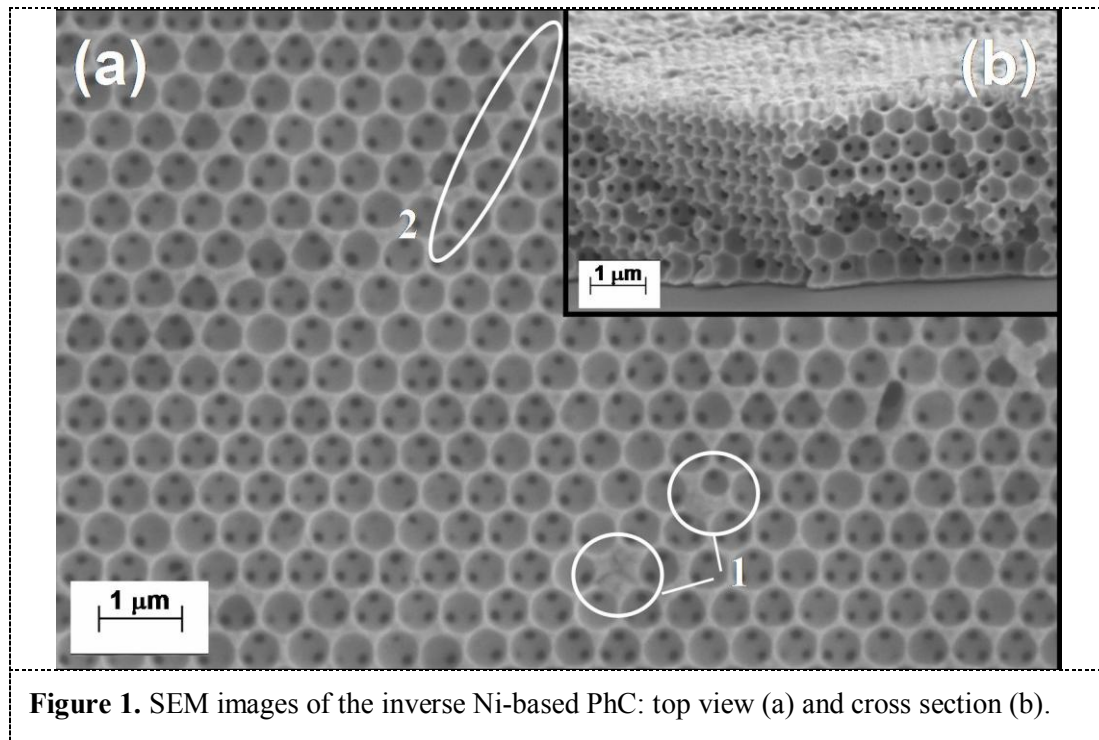


**Figure 1.** SEM images of the inverse Ni-based PhC: top view (a) and cross section (b).

One can see that the crystal surface bears point (1) and linear (2) defects, which are related to microsphere packing, as well as the cracks related to conditions of the template synthesis [4]. In addition, we observe a surface containing hexagonally ordered spherical voids. It is known that the direction perpendicular to the substrate is always the [111] axis of the FCC structure [5, 6], and the vertical axis (along which the meniscus is moving) corresponds always to the [20-2] crystallographic direction. Thus, one can get the idea of the crystal orientation as early as at the stage of synthesis.

### 3. Experiment

Microradian X-ray diffraction experiments were performed at the BM-26B Dutch-Belgian beam line (DUBBLE) of the European Synchrotron Radiation Facility (ESRF) in Grenoble, France [7-9]. The monochromatic X-ray beam with the energy  $E = 15$  keV (wavelength  $\lambda = 0.826\text{\AA}$ , size  $0.5 \times 0.5$  mm<sup>2</sup> and divergence 10 mrad) was used. Diffraction of the synchrotron radiation was registered by a two-dimensional detector (Photonic Science CCD-camera,  $4000 \times 2700$  pixels of  $22 \mu\text{m}^2$ ) positioned at a distance of  $\sim 8$  m downstream of the sample along the Y axis. To improve the resolution, the beam was focused by a set of compound beryllium lenses installed in front of the sample. This setup allows achieving an angular resolution in the order of a few microradians, which is sufficient for collecting detailed information on the structure of large period photonic crystals [10, 11]. The inverse PhC films were mounted on a goniometric head, which allows careful orientation of the sample. The 3D crystal structure is investigated by collecting the X-ray diffraction patterns for different rotation angles of the sample around its [2-20] axis in the range from  $-60$  to  $+60$  [12].

### 4. Results and discussion

The small angle diffraction of synchrotron radiation is a very efficient and distinctive way to determine the structure and to characterize the ordering degree of the inverse PhC. In the small angle

diffraction geometry the image on the detector is a section of the Fourier image of the crystal structure by the plane perpendicular to the X-ray beam. Thus, by rotating the crystal and simultaneously recording the diffraction images, one can reconstruct the 3D Fourier image [13], like in a single crystal X-ray diffraction experiment, but on the mesoscopic scale.

Experiments with microradian synchrotron diffraction were performed on the Ni inverse PhC deposited onto the conductive substrate; some of experimental images are shown in Figure 2.

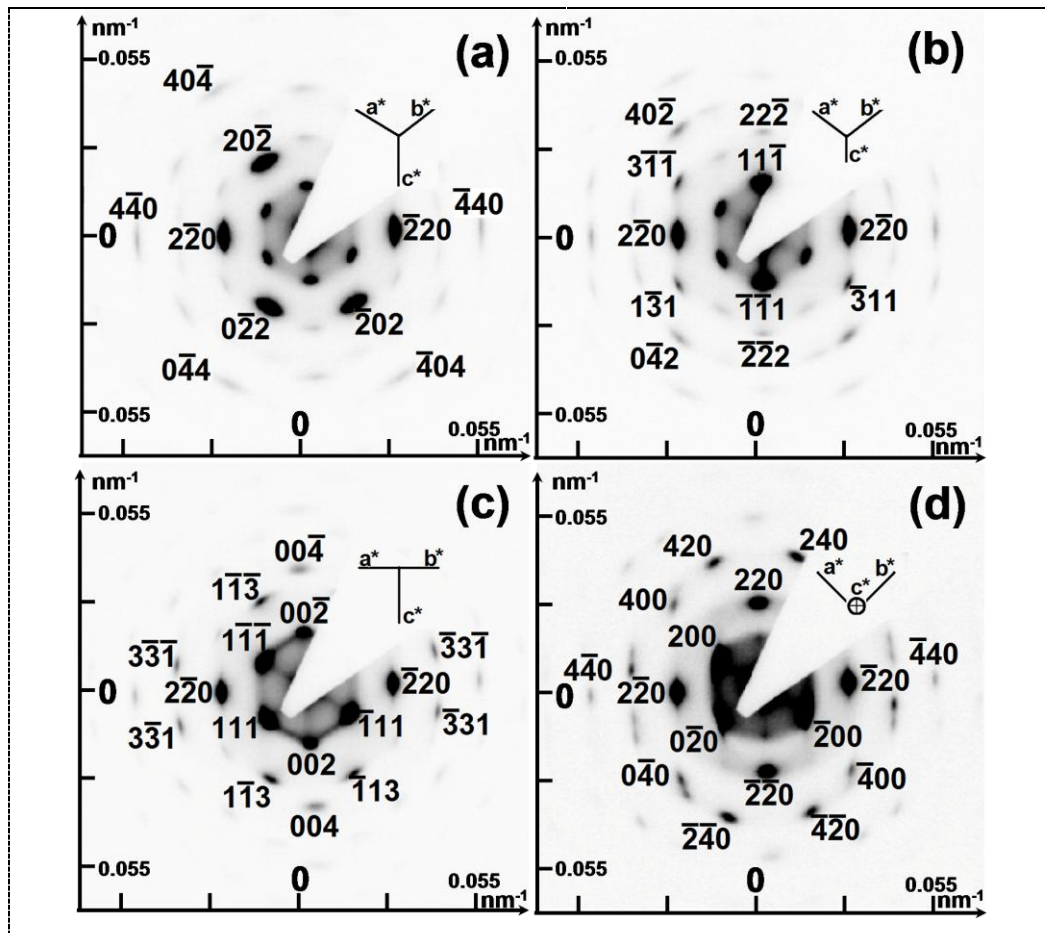
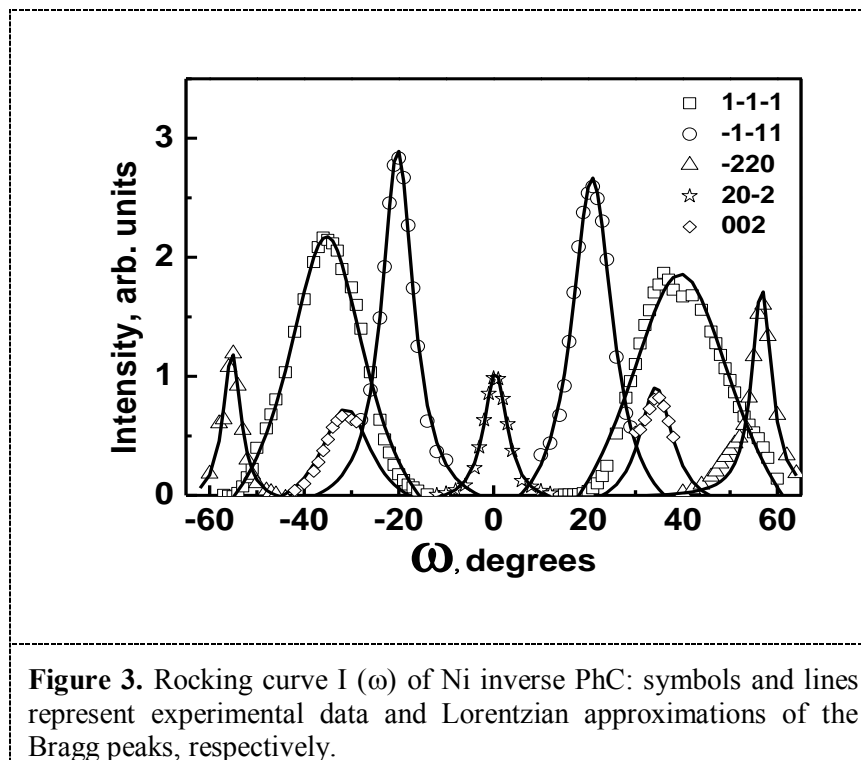


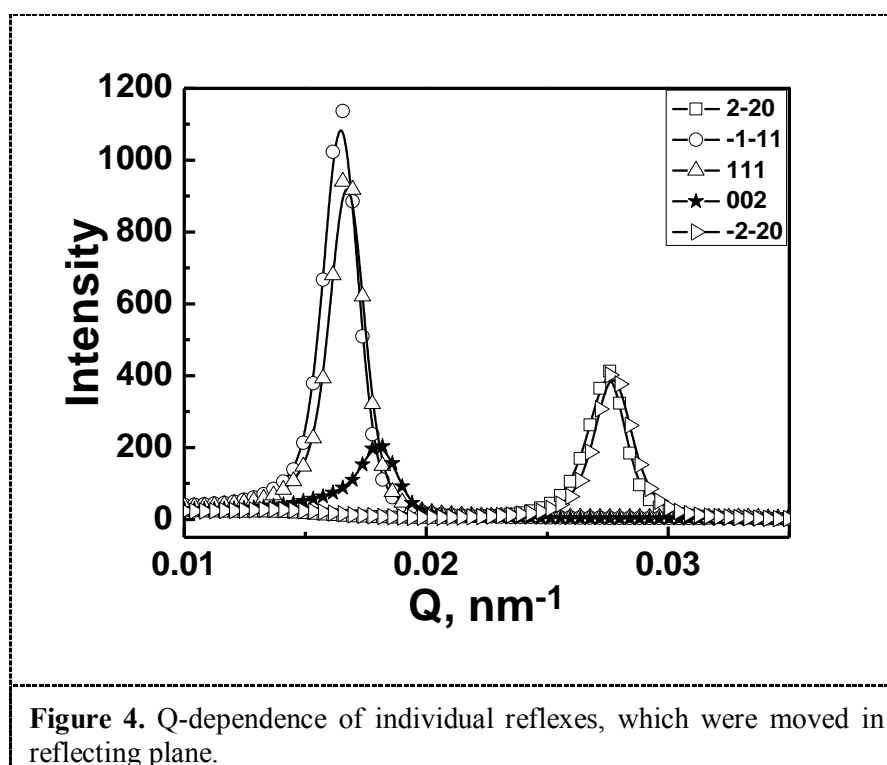
**Figure 2.** Diffraction patterns of the Ni inverse PhC at various rotation angles:  $\omega = 0^\circ$  (a),  $19^\circ$  (b),  $35^\circ$  (c),  $55^\circ$  (d) around the  $[2-20]$  axis.

The diffraction patterns were recorded at various rotation angles:  $\omega = 0^\circ, 19^\circ, 35^\circ, 55^\circ$ , where the  $[2-20]$  was the rotation axis and zero angle corresponds to the geometry of the inverse PhC surface perpendicular to the beam. These obtained pictures can be identified assuming the face-centered cubic (FCC) structure and accounting for thickness (the SEM shows that the sample consists of 8 layers only) and hexagonal fault effects. Note that peaks of the inner hexagonal rings at  $\omega = 0$  (Figure 2a) are much weaker than reflexes of the second ring, which are the  $(2-20)$  reflexes of the FCC structure. Accordingly, panels (b, c, d) show the reflection patterns for the reciprocal lattice of FCC structure cut by the  $(112)$  (b),  $(110)$  (c), and  $(100)$  (d) planes. Bragg reflexes appearing in the diffraction pictures can be identified as those belonging to the FCC structure, which is further corroborated by position of the diffraction maximum on the rocking curves (Figure 3)



Presence of two almost symmetrically positioned diffraction maxima in the rocking curves for the most of reflexes indicates that the crystal is composed from blocks with different sequences of packing layers, ABCABC- and ACBACB-type stacking [1, 14], the volume ratio those twin components can be roughly estimated from the ratio of integral intensities of Bragg reflexions and it is close to 4:5 for the considered case.

Figure 4 shows Q-dependences of individual reflexes, positions of the maxima also correspond to the FCC structure, for example  $Q_{(2-20)}^{\text{exp}} = 0.02746 \pm 10^{-5} \text{ nm}^{-1}$  and  $Q_{(2-20)}^{\text{cal}} = 0.027911 \text{ nm}^{-1}$ ,  $Q_{(11-1)}^{\text{exp}} = 0.01645 \pm 10^{-5} \text{ nm}^{-1}$  and  $Q_{(2-20)}^{\text{cal}} = 0.017092 \text{ nm}^{-1}$ , i.e. the inaccuracy is 3 %. High resolution allows us to resolve positions of the (-1-11) and (002) reflections (Fig.4), although they are located close to each other. Note that the experimentally observed ratio of intensities well coincides with the theory, according to which the (002) reflexes appear to be orders of magnitude weaker than the (111) or (220) reflexes. The lattice constant of Ni inverse PhC is  $650 \pm 10 \text{ nm}$ .



The spatial extent of the periodic order could be derived from the full width at half maximum  $\Delta Q$  of the diffraction peaks, which can be determined either from a single diffraction pattern (for lateral periodicity) or from the rocking curves (for the periodicity along the beam). The transverse structural correlation length (perpendicular to the scattering vector  $Q$ )  $L_{tran}$  has been calculated using the equation:  $L_{tran} = 2\pi/(Q_{(2-20)} \sin\Omega)$ , when  $Q_{(2-20)}$  is the position of reflex (2-20) in  $\text{nm}^{-1}$ ,  $\Omega$  is the FWHM of reflection. This transverse structural correlation length  $L_{coh}$  defined from the rocking curves is  $2.4 \pm 0.1 \mu\text{m}$ , which corresponds to a sample thickness of order of 6 layers, which is two layers smaller than that obtained from the SEM image in Fig.1. One can not pretend to give the exact number of layers obtained from the coherent length but the qualitative agreement has been clearly achieved. The structural correlation length (longitudinal along the  $Q$ ) obtained from the value of FWHM according to the formula  $L_{long} = 2\pi/\Delta Q$  is  $3.4 \pm 0.2 \mu\text{m}$ . The mosaicity, i.e. mis-orientation of ABC- ACB- domains within the sample, is of order of  $\delta\phi = 10^\circ$ . Thus, the degree of disorder has been described by the three parameters: transverse correlation length  $L_{long}$ , structural correlation length  $L_{tran}$ , and mosaic spread  $\delta\phi$  of the structure.

## Conclusions

The data presented here show that the electrochemical method of synthesis, indeed, allows one to duplicate the structure of artificial opals and to obtain the inverse photonic crystal. The crystals have predominantly FCC structure with the lattice constant being  $650 \pm 10 \text{ nm}$  and of average size of coherent block about few microns. Among many methods to characterize photonic crystals, the microradian X-ray diffraction of synchrotron radiation provides the most detailed information on average structure, disorder phenomena, and structural coherence. The first two characteristics are normally expressed in terms of certain type of dense-packing structure and stacking defects and diffraction experiment becomes necessary metrological components of photonic crystallography. The last portion of diffraction data, namely, is shape and size of Bragg nodes, seems to be of a lesser use



for now. We show that even very simple analysis presented here provides the unique information on the size of structurally coherent crystal blocks. It would be very interesting for a future study to monitor the dependence of structural coherence on materials and technological parameters of fabrication of inverse photonic crystals.

### Acknowledgment

The Russian authors thank for partial support the Russian Foundation of Basic Research (Grant No 10-02-00634) and the Federal Special Program of Russian Federation (Projects Nos. 02.740.11.5186). This work is also supported by the Presidium of the Russian Academy of Sciences under the Program for Basic Research and the Programs of the High School of Russian Federation 2.1.1/4661 and “Michail Lomonosov II”. We thank The Netherlands Organisation for Scientific Research (NWO) for the access provided to a synchrotron X-ray beamline and K. Kvashnina and D. Detollenaere, station staff members of the Dutch–Belgian Beam Line (ESRF-DUBBLE), for assistance in the synchrotron X-ray experiment.

### References

- [1] Hilhorst J, Abramova V V, Sinitiskii A, Sapoletova N A , Napolskii K S, Eliseev A A, Byelov D V, Grigoryeva N A , Vasilieva A V, Bouwman W G, Kvashnina K, Snigirev A, Grigoriev S V , and Petukhov A V 2009 *J Langmuir* **25** 10408
- [2] Napolskii K S , Sapoletova N A , Gorozhankin D F, Eliseev A A, Petukhov A V, Byelov D V, Mistonov A A, Grigoryeva N A, Bouwman W G, Kvashnina K, Snigirev A, Chernyshov D Yu , Vasilieva A V, Grigoriev S V 2009 *J Langmuir* in print DOI: 10.1021/la902793b
- [3] Kuai Su-Lan, Hu X-F, Hache A, Truong Vo-Van 2004 *J of Crystal Growth* **267** 317
- [4] Plekhanov A I, Kalinin D V, Serdobintseva V V 2006 *J Rossiiskie nanotekhnologii* **1** 245
- [5] Baryshev A V, Kosobukin V A, Samusev K B, Usvyat D E, and Limonov M F 2006 *J Phys. Rev. B* **73**, 205118
- [6] Gasperino D, Meng L, Norris D J, Derby J J 2008 *J of Crystal Growth* **310** 131–139
- [7] Borsboom M, Bras W, Cerjak I, Detollenaere D, van Loon D G, Goedtkindt P, Konijnenburg M, Lassing P, Levine Y K, Munneke B, Oversluizen M, van Tol R and Vlieg E 1998 *J Synch Rad* **5** 518
- [8] Bras W, Dolbnya I P, Detollenaere D, van Tol R, Malfois M, Greaves G N, Ryan A J and Heeley E 2003 *J Appl Cryst* **36** 791
- [9] Nikitenko S, Beale A M, van der Eerden A M J, Jacques S D M, Leynaud O, O'Brien M G, Detollenaere D, Kaptein R, Weckhuysen B M and Bras W 2008 *J Synch Rad* **15** 632
- [10] Grigoriev S V, Napolskii K S, Grigoryeva N A, Vasilieva A V, Mistonov A A, Chernyshov D Yu, Petukhov A V, Byelov D et al 2009 *J Phys Rev B* **79** 045123
- [11] Thijssen J H J, Petukhov A V, 't Hart D C, Imhof A, van der Werf C H M, Schropp R E I, and van Blaaderen A 2006 *J Adv Mater* **18** 1662
- [12] Grigoriev S V, Napolskii K S, Grigoryeva N A, Vasilieva A V, Mistonov A A, Chernyshov D, Petukhov A V, Belov D V et al, 2009 *J Phys Rev B* **79** 045123
- [13] Eliseev A A, Gorozhankin D F, Napolskii K S, Petukhov A V, Sapoletova N A, Vasilieva A V, Grigoryeva N A, Mistonov A A, Byelov D V, Bouwman W G, Kvashnina K O, Chernyshov D Yu, Bosak A A and Grigoriev S V 2009 *JETP Lett* **90** 272
- [14] Abramova V V, Sinitiskii A S, Grigor'eva N A, Grigor'ev S V, Belov D V, Petukhov A V, Mistonov A A, Vasil'eva A V and Tret'yakov Yu D 2009 *JETP* **109** 29